Developmental Cell, Volume *46*

Supplemental Information

Tdrd6a Regulates the Aggregation of Buc into Functional Subcellular Compartments that Drive Germ Cell Specification

Elke F. Roovers, Lucas J.T. Kaaij, Stefan Redl, Alfred W. Bronkhorst, Kay Wiebrands, António M. de Jesus Domingues, Hsin-Yi Huang, Chung-Ting Han, Stephan Riemer, Roland Dosch, Willi Salvenmoser, Dominic Grün, Falk Butter, Alexander van Oudenaarden, and René F. Ketting

Supplemental Figure 1

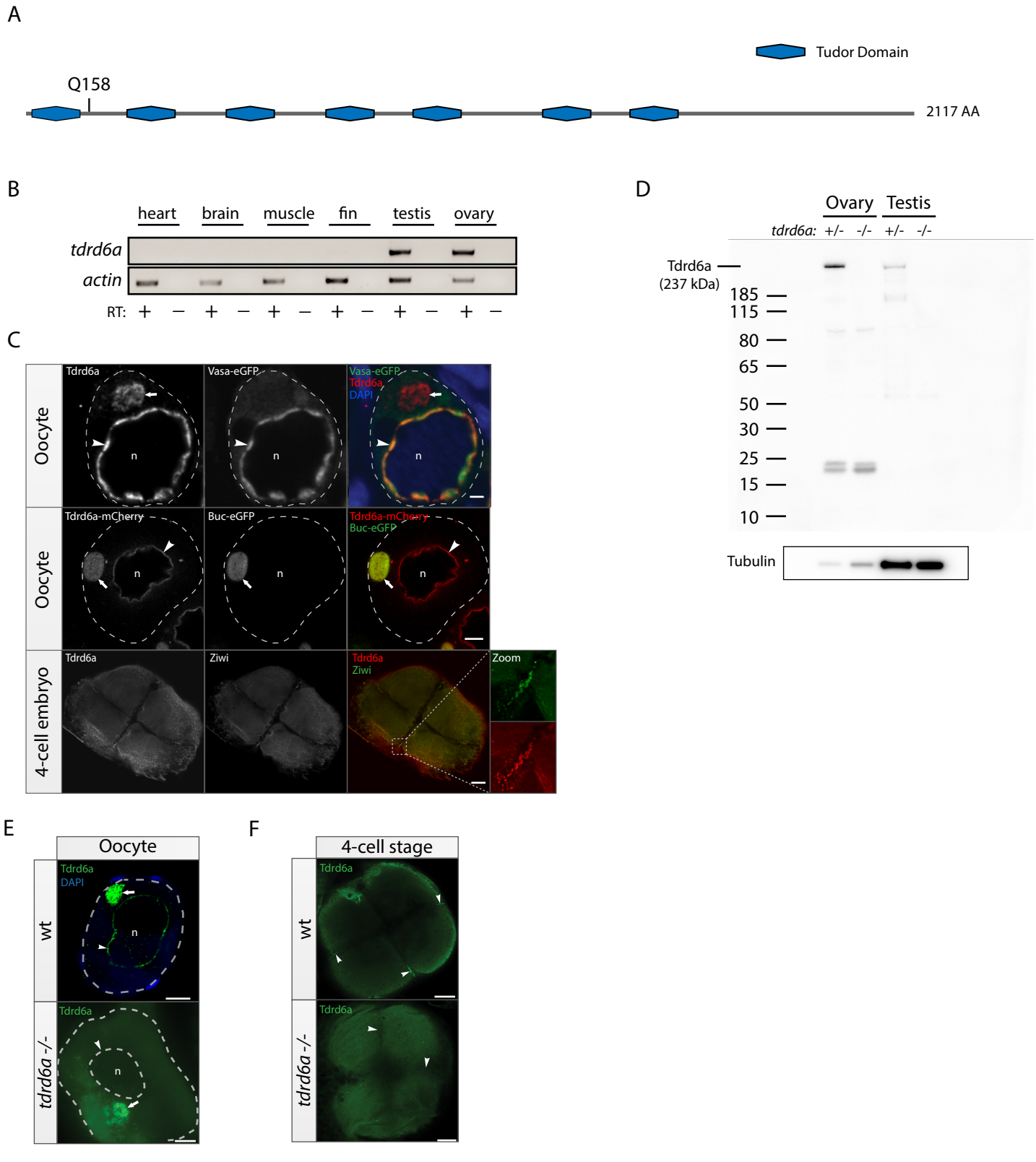

Supplemental Figure 2

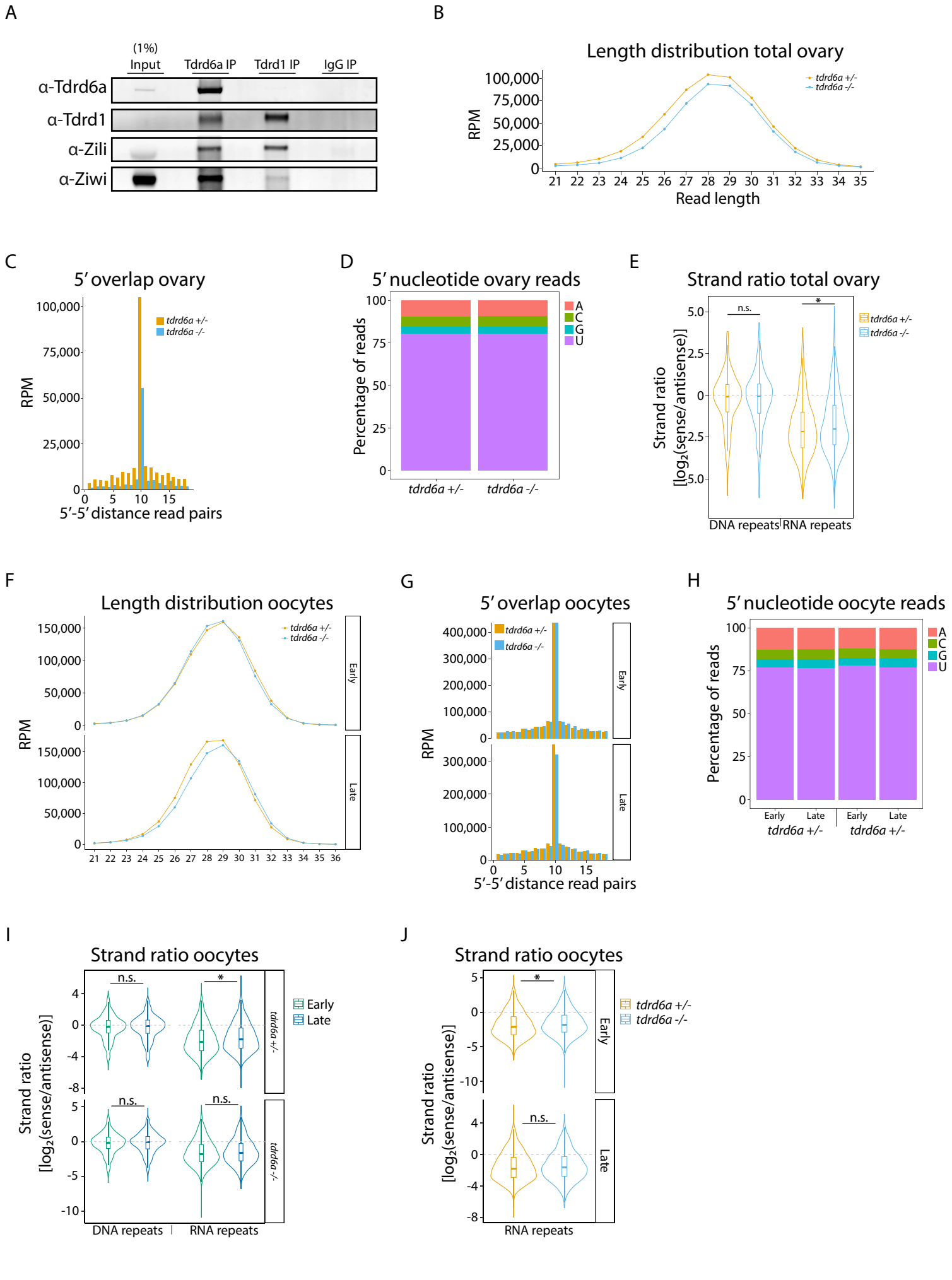

Supplemental Figure 3

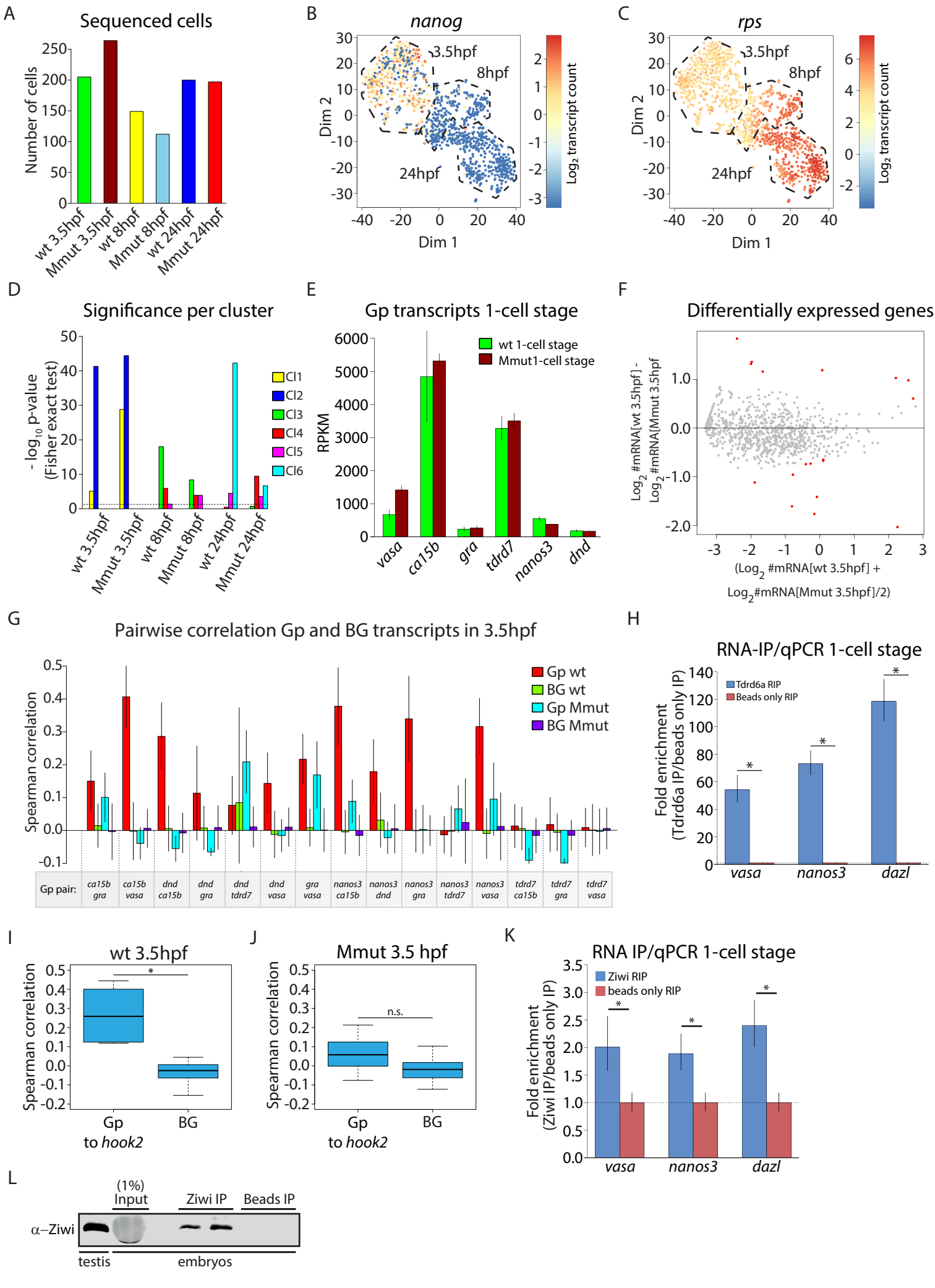

Supplemental Figure 4

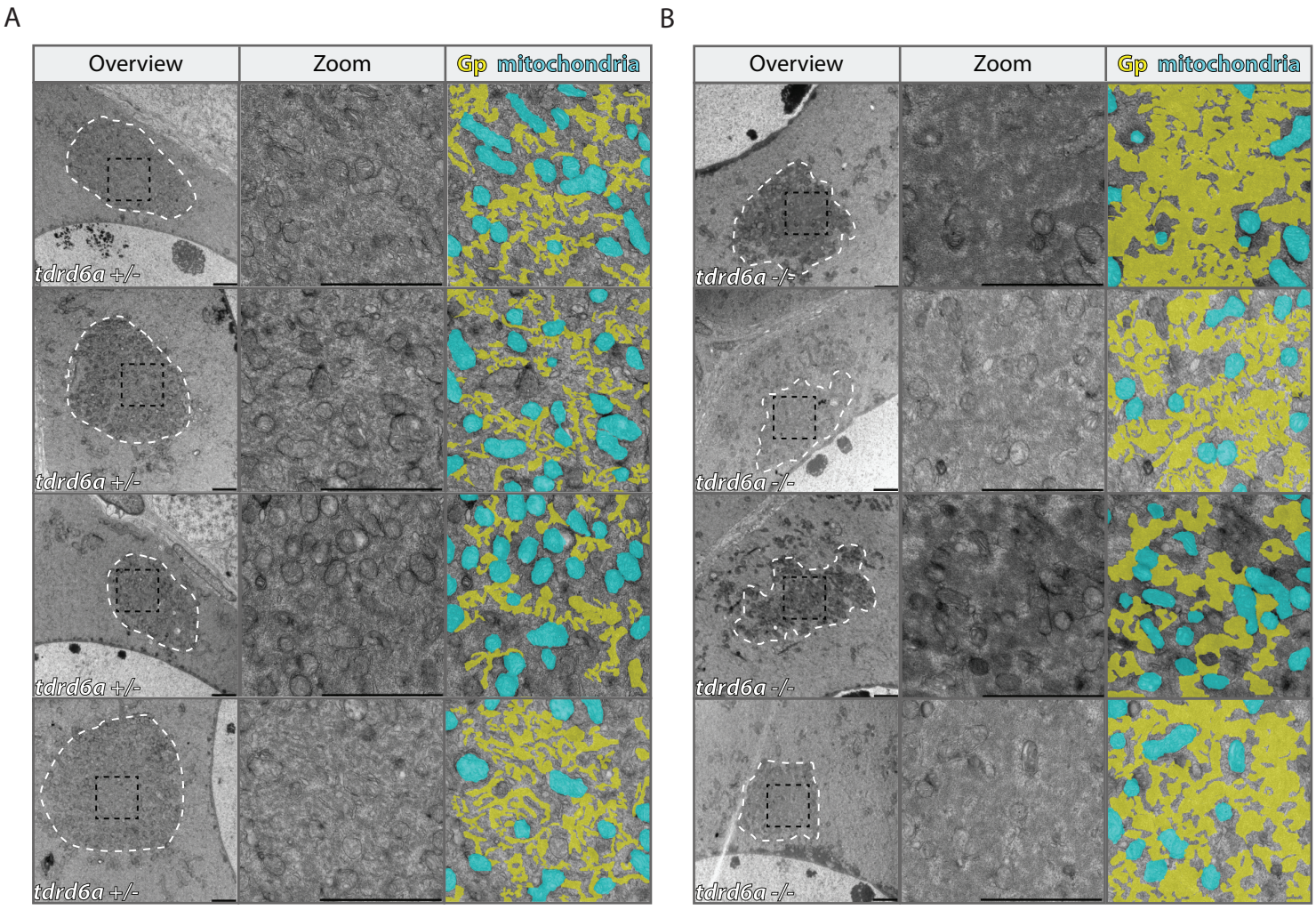

Supplemental Figure 5

A

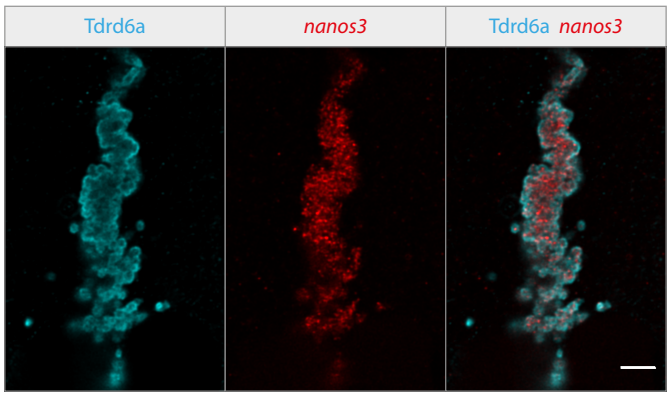

B

Supplemental Figure 6

A

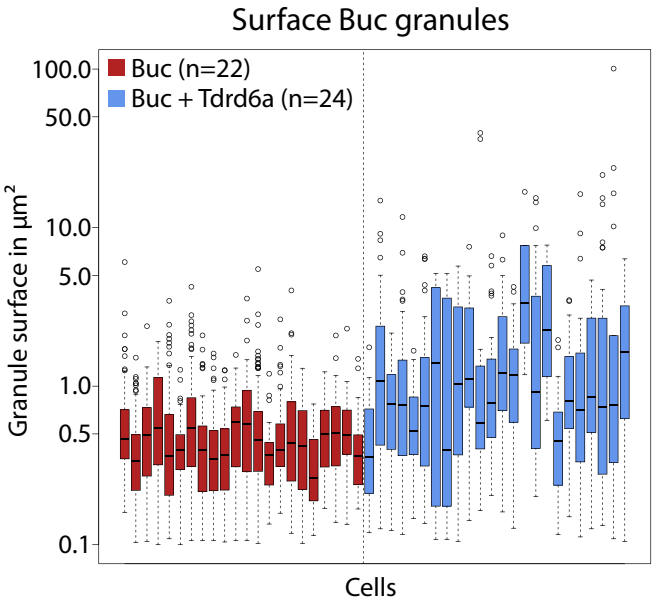

B

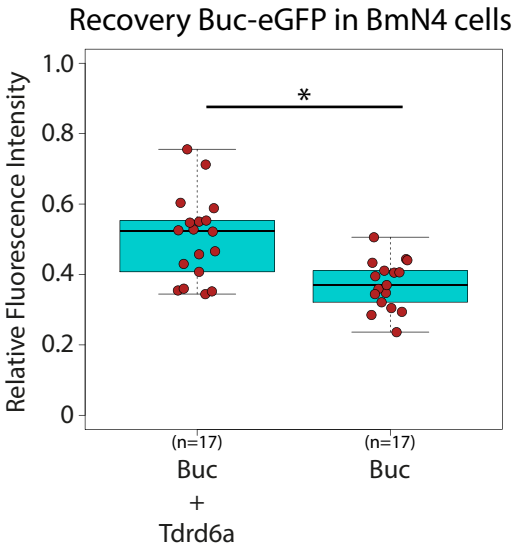

C

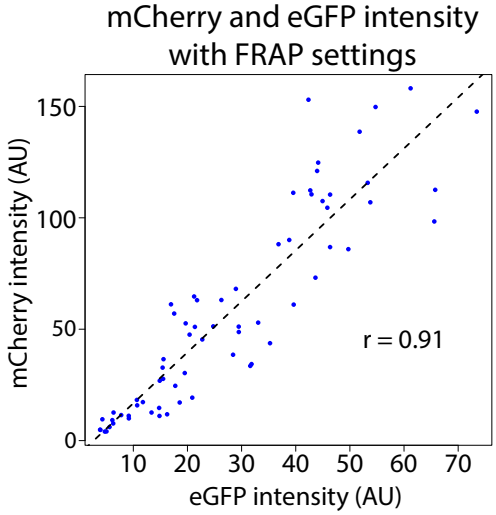

Supplemental Figure 7

A

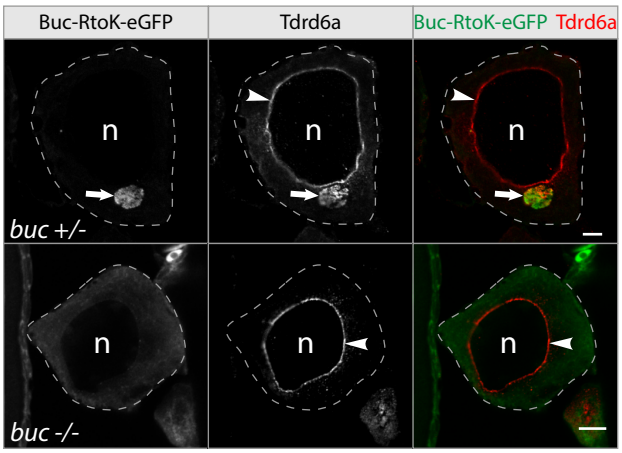

B

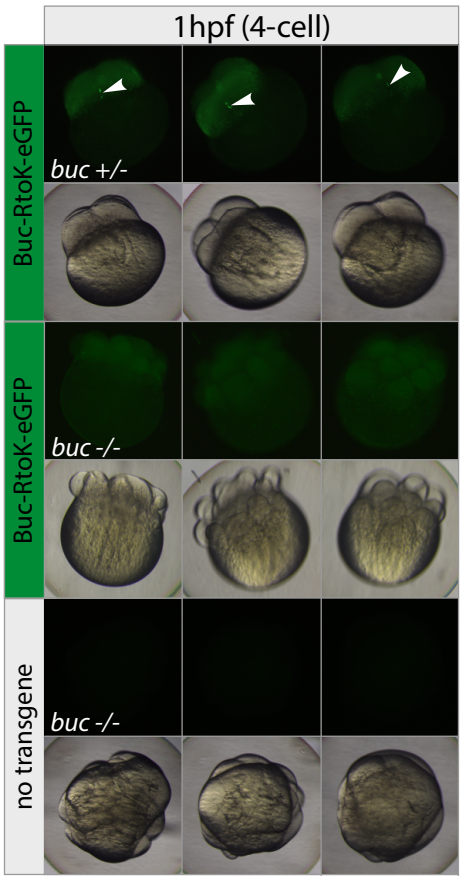

Supplemental Figure 1, Related to Figure 1. (A) Schematic overview of Tdrd6a. (B) RT-PCR of different tissues to confirm germline expression. (C) Tdrd6a co-localizes to Vasa-eGFP in nuage, to Buc-eGFP in the Bb (Riemer et al., 2015) and to Ziwi in the Gp. A Tdrd6a-mCherry-polyA3'UTR was used under a Ziwi promoter, which expresses until ~stage II oocytes. Scale bars (top-middle-bottom): 2µm, 10µm and 100µm (D) Western blot for Tdrd6a in wt and *tdrd6a-/-* ovary and testis. (E) Tdrd6a staining in wt and *tdrd6a* mutant ovary. Tdrd6a is lost from nuage in the *tdrd6a* mutant (arrowhead) but some signal from the Bb remains (arrow). Wt is taken along from Figure 1A for comparison. Scale bars indicate 10µm (F) Tdrd6a staining in wt and a MZ *tdrd6a* mutant 4-cell stage embryo. Arrowheads indicate the cleavage planes. Wt is taken along from Figure 1B for comparison. Scale bars indicate 100µm.

Supplemental Figure 2, Related to Figure 1. (A) Quantitative Western blot for Tdrd6a, Tdrd1 and IgG IPs (based on IRDye detection with LI-COR). Ziwi is 3.3x more present in Tdrd6a IPs compared to Tdrd1 IPs, when normalized to Zili. (B) Length distribution sRNA reads mapping to TEs for *tdrd6a+/-* and *tdrd6a-/-* ovary, as indicated. (C) 5' overlap of piRNAs in *tdrd6a+/-* and *tdrd6a-/-* ovary. Ping-pong Z-scores are 39 and 41 for *tdrd6a +/-* and *tdrd6a -/-* respectively. (D) 5' nucleotide bias displaying the typical 5'U bias in both genotypes. (E) The sense/antisense bias observed in ovary of *tdrd6a+/-* and *tdrd6a-/-* siblings is plotted for all DNA and RNA transposons. *Tdrd6a -/-* ovary shows a reduction in antisense piRNAs ($p = 0.03$) mapping to RNA elements. (F) Length distribution sRNA reads mapping to TEs for *tdrd6a+/-* and *tdrd6a-/-* early and late oocytes, as indicated. (G) 5' overlap of piRNAs in *tdrd6a+/-* and *tdrd6a-/-* early and late oocytes. Ping-pong Z-scores are 30 and

32 in early oocytes and 32 and 33 in late oocytes, for *tdrd6a+/-* and *tdrd6a -/-* respectively. (H) 5' nucleotide bias displaying an unaffected 5'U bias. (I,J) The sense/antisense bias observed in ovary of *tdrd6a+/-* and *tdrd6a-/-* siblings plotted for reads mapping against DNA and RNA transposons, early versus late (I) and *tdrd6a +/-* versus *tdrd6a -/-* (* indicates $p < 0.01$, Mann-Whitney-Wilcoxon Test) (J) RPM = Reads per million.

Supplemental Figure 3, Related to Figure 2. (A) Barplot displaying the number of cells per genotype and developmental timepoint used in this study. (B and C) t-SNE maps showing transcript counts of *nanog* and the *rps* gene group, respectively. (D) Barplot displaying the significance of enrichment for the different genotype-developmental time combinations in the six clusters identified in (2B). (E) Barplot displaying the RPKM counts for six Gp mRNAs from bulk RNA-seq of 1-cell stage wt and Mmut *tdrd6a* embryos, as indicated. Error bars indicate standard deviation obtained from three biological replicates. (F) Scatterplot displaying transcript counts in wt and Mmut PGCs at 3.5hpf based on scRNA-seq. Genes highlighted in red are 2 fold up or down regulated between genotypes with a p-value < 0.01 (p-value is calculated by negative binominal statistics and corrected for multiple testing (Benjamini–Hochberg)). (G) Barplot representing the Spearman correlation between Gp-Gp transcript and BG-BG transcripts in 3.5hpf old embryos, as indicated. Standard deviations of the Gp-Gp correlations were obtained by bootstrapping. (H) Tdrd6a RIP-qPCR analysis for *nanos3*, *dazl* and *vasa*. Enrichments were calculated compared to beads only RIP and normalized to *β-actin*. Error bars represent standard deviation of two biological replicates (* indicates p-value < 0.001, p-value obtained by two-sided Student's t-test). (I, J) Boxplots displaying the *hook2*-Gp and BG-BG correlations in 3.5hpf PGCs form wt and Mmut embryos, as indicated (* = p-value < 0.001, n.s. = non-significant, calculated by Wilcoxon test). (K) Ziwi

RIP-qPCR analysis for *nanos3*, *dazl* and *vasa*. Enrichments were calculated compared to beads only RIP and normalized to *β-actin*. Error bars represent standard deviation of two biological replicates (* = p-value < 0.05, p-value obtained by two-sided Student's t-test). (L) Western blot control for successful IP of (K).

Supplemental Figure 4, Related to Figure 3. (A, B) Additional electron micrographs to further illustrate *tdrd6a* heterozygous (A) and mutant (B) Balbiani bodies, including the Bbs from Figure 3E and F (bottom row). Overlays in the right panel indicate the Gp regions (yellow) and mitochondria (cyan) that can be appreciated in the middle panel.

Supplemental Figure 5, Related to Figure 4. (A) FISH against *nanos3* using anti-DIG IHC combined with Tdrd6a IHC visualizing Gp at a 4-cell stage embryo cleavage plane. (B) Maximum projections of Z-stacks of wt and Mmut Gp of 4-cell stage Buc-eGFP signals, used to calculate Gp volumes of Figure 4C. Red dotted line indicates the largest Gp fragment, of which the volume in in μm^3 was measured. Scalebars represent 5µm (A) and 10µm (B).

Supplemental Figure 6, Related to Figure 6. (A) Surface calculation of Buc-containing granules in transfected BmN4 cells in μm^2. Overall, granules increase in size in the presence of Tdrd6a, with large variation between co-transfected cells. (B) Boxplot of the recovery of separate FRAP experiments of Buc-eGFP as in Figure 6E, based on the average intensity value of the last 20 frames (* indicates p-value < 0.05, calculated by Wilcoxon test). (C) Fluorescence intensity of an mCherry-eGFP fusion construct as indicated, using the FRAP settings used in Figure 6E.

Supplemental Figure 7, Related to Figure 7. (A) Tdrd6a localization in sections of *buc+/-* and *buc-/-* oocytes in the Buc-RtoK-eGFP background. Arrow: Bb, arrowheads: nuage. Scale bar represents 10μm (B) Examples of 4-cell stage embryos of *buc +/-* and *-/-* mothers, with and without Buc-RtoK-eGFP. Without the presence of wt Buc, Buc-RtoK can rescue the lack of polarity of the *buc* phenotype (*buc -/-*, no transgene), even though most embryos display severe developmental defects (*buc -/-*, Buc-RtoK-eGFP). Arrowheads: Gp.